

# *msl2* mRNA is bound by free nuclear MSL complex in *Drosophila melanogaster*

Anna-Mia Johansson<sup>1</sup>, Anders Allgardsson<sup>1</sup>, Per Stenberg<sup>1,2</sup> and Jan Larsson<sup>1,\*</sup>

<sup>1</sup>Department of Molecular Biology, Umeå University, SE-90187 Umeå and <sup>2</sup>Computational Life Science Cluster (CLiC), Umeå University, Sweden

Received February 4, 2011; Revised March 14, 2011; Accepted April 4, 2011

## ABSTRACT

In *Drosophila*, the global increase in transcription from the male X chromosome to compensate for its monosomy is mediated by the male-specific lethal (MSL) complex consisting of five proteins and two non-coding RNAs, *roX1* and *roX2*. After an initial sequence-dependent recognition by the MSL complex of 150–300 high affinity sites, the spread to the majority of the X-linked genes depends on local MSL-complex concentration and active transcription. We have explored whether any additional RNA species are associated with the MSL complex. No additional *roX* RNA species were found, but a strong association was found between a spliced and poly-adenylated *msl2* RNA and the MSL complex. Based on our results, we propose a model in which a non-chromatin-associated partial or complete MSL-complex titrates newly transcribed *msl2* mRNA and thus regulates the amount of available MSL complex by feedback. This represents a novel mechanism in chromatin structure regulation.

## INTRODUCTION

Dosage compensation in *Drosophila* provides one of the best examples of chromosome-wide gene regulation (1,2). The compensation mechanism must fulfil two requirements. It must balance the relative expression between sex chromosomes and autosomes and also equalize the transcriptional activities of the two X chromosomes in the homogametic sex with that of the single X chromosome in the heterogametic sex. Examination of X-linked and autosomal gene expression in *Drosophila*, *Caenorhabditis elegans* and mammals has revealed that X-linked genes are expressed, on average, twice as strongly as autosomal genes (3–5), implying that dosage compensation involves compensation of X chromosome

expression not only between the two sexes, but also in relation to the expression of autosomes. Thus, X inactivation in mammals might be considered as a response in females to the overexpression of the X chromosome. This overexpression is required by males because they have just one X chromosome.

The male restricted 2-fold increase of X chromosome gene expression in *Drosophila* fulfils both compensation requirements described above. This seems to be mediated by a general buffering mechanism for all monosomic regions, resulting in an ~1.4-fold expression increase (6–8) followed by an ~1.35-fold expression increase restricted to the X chromosome, mediated by the MSL complex (7–10). In *Drosophila melanogaster*, two non-coding RNAs, *roX1* and *roX2*, have been shown to be essential components of the dosage compensation system. Together with at least five MSL proteins, *roX1* and *roX2* form male-specific lethal (MSL) complexes that ‘paint’ the male X chromosome, and mediate acetylation of H4 at lysine 16 on the male X chromosome, which partly explains its subsequent hypertranscription (2,11). Recent data suggest that the MSL complex, in addition, have intrinsic properties that constrain the activation potential of MOF (males absent on the first) to end up with the required 2-fold activation (12). The prevailing model of the targeting process is that the MSL complex is recruited to a set of 150–300 high-affinity MSL recognition elements (MRE) in a sequence-depending mechanism (13). Subsequent spreading to neighboring genes with lower affinities depends on the local MSL-complex concentration (14), X chromosome location (15) and active transcription (16,17). The sequence dependence of the spreading remains poorly understood. Irrespective of differences in transcript levels of genes and the transcription requirements of different cells, a 2-fold transcriptional up-regulation is required.

MSL2 protein is the limiting component for the formation of the MSL complex. In females, translation of *msl2* mRNA is inhibited by the binding of the Sex lethal (Sxl) protein in both the 5' and the 3'-UTRs (18–20). Overexpression of *msl2* is toxic to females and becomes

\*To whom correspondence should be addressed. Tel: +46 (0)90 7856785, Fax: +46 (0)90 778007, Email: jan.larsson@molbiol.umu.se

lethal for females and toxic to males in combination with the overexpression of *msl1*, again highlighting the requirement for correct concentrations of the MSL complex (12,19,21,22). Furthermore, association studies suggest that MSL2 levels are tuned to match those of the other MSL-complex components (23).

Although the *roX* genes are important for correct targeting of the MSL complex, in *roX1 roX2* double mutants escaping males are recovered (22,24,25). This contrasts with the absence of escaper males when the *msl* genes are mutated. The partial viability of *roX1 roX2* double mutants could be explained by the presence of additional *roX* RNA species (26,27), even though unsaturated screens have failed to isolate such species (27,28). It has also been hypothesized that MSL complex may bind to additional RNAs produced by cryptic transcription as a mediator of spreading (26).

Here we have used RNA-immunoprecipitation (RIP) followed by tiling array analysis to determine the association between the MSL complex and RNA moieties. We found no additional ncRNA associated to the complex. However, we observed a strong association between the *msl2* mRNA and a non-chromatin-associated MSL complex. These data suggest a novel mechanism in chromatin structure regulation in which a non-chromatin-associated form of a chromatin regulatory complex attracts an intrinsic rate-limiting mRNA and thus regulates the amounts of the complex available for chromatin targeting by feedback.

## MATERIALS AND METHODS

### Immunostaining and *in situ* hybridization of polytene chromosomes

Polytene chromosomes from the salivary glands of third-instar larvae were prepared and stained essentially as previously described (29). Salivary glands were fixed in 2% formaldehyde in PBS, 0.1% Triton X-100, 0.2% NP-40 for 40 s followed by 2–3 min in 50% acetic acid, 1% formaldehyde. Polytene chromosomes were squashed as previously described (30). The slides were washed for 30 min in 1× PBS, 0.1% Triton X-100, transferred to blocking solution (0.1 M maleic acid, 0.15 M NaCl, 1% Boehringer blocking reagent) and incubated for 30 min at room temperature. The slides were then incubated overnight at 4°C with primary antibody raised against MSL2 (1:300), MSL3 (1:2000) or MLE (1:2000). The slides were washed 2× 10 min in 0.1 M maleic acid, 0.15 M NaCl, 0.3% Tween-20 and blocked for 30 min. Donkey anti-rabbit and anti-goat (Jackson Laboratories) conjugated with Cy3 or FITC (diluted 1:400) were used as secondary antibodies and incubated at room temperature for 2 h. The squashes were counterstained with DAPI (1 µg/ml) and washed 2× 10 min before mounting with Vectashield (Vector). Preparations were analyzed using a Zeiss Axiophot microscope equipped with a KAPPA DX20C charge-coupled device camera. Images were assembled and merged electronically using Adobe Photoshop. For *in situ* hybridization, the slides were prepared as above and hybridized and washed essentially

as previously described (31). The slides were hybridized against a DIG-labeled antisense RNA probe against *roX1* (GH10432) or *msl2* (GH22488). The DIG-labeled probe was detected using sheep anti-Digoxigenin (0.4 µg/ml, Roche) followed by donkey-anti-sheep conjugated with AlexaFluor555 (Molecular Probes, diluted 1:500) and DAPI counterstaining. *roX1 roX2* double mutant males were selected as non-GFP males from a *yw roX1<sup>ex6</sup> Df(1)roX2<sup>52</sup> P[w<sup>+</sup>4A4.3] FM7i, P[w<sup>+</sup>mC ActGFP]/JMR3* stock. Females and males overexpressing *msl2* were selected from a *w; P[w<sup>+</sup> hsp83:msl2] msl3/TM6B* stock.

### Immunostaining and *in situ* hybridization of S2-cells

Schneider's line 2 cells (ATCC CRL-1963) were grown as a suspension culture at 25°C in Erlenmeyer flasks to a density of  $1 \times 10^7$  cells/ml in *Drosophila* SFM medium (Invitrogen), supplemented with 100 U/ml Penicillin G, 100 µg/ml Streptomycin sulfate and 2 mM of L-glutamine.  $0.2 \times 10^7$  cells were placed on Polysine slides (VWR) and incubated at room temperature for 1 h. The cells were fixed for 10 min with 2% formaldehyde in PBS and permeabilized with 0.1% Triton X-100 in PBS for 10 min at room temperature. The slides were washed twice in 70% ethanol before dehydration at 80, 95 and 99.5% ethanol and then air dried. The slides were hybridized and washed as described above using DIG-labeled antisense RNA probes against *roX1* (GH10432), *roX2* (GH18991), *msl2* (GH22488) or *CkIIB* cDNA and immunostained in parallel with anti-MSL1 (1:500).

### RIP-chip

For each sample treatment condition, we used 300 ml cultured *D. melanogaster* Schneider's line 2 cells. The cells were pelleted, washed twice in 100 ml 10 mM HEPES pH 7.4, 140 mM NaCl and resuspended in 50 ml of lysis buffer (20 mM HEPES pH 7.4, 3 mM MgCl<sub>2</sub>, 0.1% Triton X-100, 1 mM dithiothreitol, 0.5 mM PMSF, 10 U/ml RNasin and 0.5× complete protease inhibitor cocktail, Roche). The cells were allowed to swell on ice for 10 min and then homogenized on ice with 30 strokes of a Dounce homogenizer. The nuclei were pelleted at 2000g for 5 min and used either as native samples (non-cross-linked) or after formaldehyde cross-linking. For the cross-linked sample (FA), the pelleted nuclei were resuspended in 50 ml lysis buffer and cross-linked by adding formaldehyde to a final concentration of 0.5% and incubated for 10 min at room temperature. The cross-linking was stopped by adding glycine (final concentration 0.125 M), the nuclei were washed once in lysis buffer and resuspended in 2 ml of sonication buffer (20 mM HEPES pH 7.4, 10% glycerol, 0.1 M NaCl, 1 mM MgCl<sub>2</sub>, 0.1% Triton X-100, 1 mM dithiothreitol, 0.5 mM PMSF, 10 U/ml RNasin and 0.5× Protease inhibitor cocktail) and sonicated using a Bioruptor (Diagenode) for 4 min at high setting (30 s ON, 30 s OFF). For the native samples the pelleted nuclei were resuspended in 2 ml sonication buffer and sonicated for 1, 3 or 6 min (N1, N3 and N6, respectively). Cellular debris was removed by

centrifugation at 14 000g for 25 min at 4°C and the supernatants were used for immunoprecipitations.

For immunoprecipitation, 1–2 mg nuclear extracts were incubated with 5 µl anti-MSL2, 5 µl anti-MOF or no antibody for 45 min at 4°C, with agitation. The antibody complexes were precipitated by incubation with 75 µl of Dynabeads conjugated to protein-A (Invitrogen) for 30 min at 4°C, with agitation. The supernatant was removed and the beads were washed twice with PBS (150 mM NaCl), 0.1% Triton X-100, 32 U/ml RNasin, 0.5× Protease inhibitor cocktail and twice in PBS (300 mM NaCl), 0.1% Triton X-100, 32 U/ml RNasin, 0.5× Protease inhibitor cocktail. The cross-linking in FA samples was reversed by adding 200 µl 0.45 M LiCl to the beads and incubating for 3–4 h at 65°C. RNA was isolated using TRI-reagent (Ambion), followed by purification using an RNeasy kit (Qiagen) according to the instructions by the suppliers. The RNA samples were concentrated and reverse-transcribed into cDNA using random primers with an ImPromII first-strand synthesis kit (Promega). The single-stranded cDNA was purified with a QIAquick PCR purification Kit (Qiagen) then the purified cDNA samples were amplified using a WGA2 GenomePlex Complete whole genome amplification kit (Sigma), according to the manufacturer's recommendations.

For tiling array analysis, amplified DNA samples were fragmented, labeled and hybridized to an Affymetrix *Drosophila* Genome 2.0 array. The signal intensity data were analyzed with the Affymetrix Tiling Analysis Software (v. 1.1.02) using 90 bp bandwidth and perfect match only. For absolute amount analysis (transcript profile), the bandwidth was set to zero. RNA enrichment ratios for all genes in nuclear extract N6 were calculated as the average enrichment ratio value of all probes located within exons of each gene. Total amounts of nuclear gene transcript were calculated from the corresponding input sample as the average value of all probes located within exons of each gene. Only genes with at least 10 probes within exons were included. For the comparison of our RIP profiles to MSL-complex binding profile the ChIP-chip data for MSL1, MSL3 and MOF from (32) were downloaded from the ArrayExpress database (accession number M-EXP-1508). The signal intensity data were analyzed with the Affymetrix Tiling Analysis Software (v. 1.1.02) using parameters: 300 bp bandwidth and perfect match only. The data were converted to *D. melanogaster* genomic release 5 using the Coordinates Converter Tool at FlyBase (33).

### RIP-qPCR

Three biological replicates of native nuclear preps from Schneider's line 2 cells (ATCC CRL-1963) were prepared as described above. The nuclei were washed once in lysis buffer and fractionation into nucleoplasm and chromatin was done essentially as described in (34). The pelleted nuclei were resuspended in 2 ml nuclear lysis buffer (20 mM HEPES pH 7.9, 3 mM EDTA, 10% glycerol, 150 mM KAc, 1.5 mM MgCl<sub>2</sub>, 0.1% Triton X-100, 1 mM dithiothreitol, 0.5 mM PMSF, 20 U/ml

RNasin and 1× Protease inhibitor cocktail) and centrifuged at 14 000g for 30 min at 4°C. The supernatant was collected as the nucleoplasmic fraction. The pelleted chromatin was resuspended in 2.8 ml of nuclear lysis buffer and solubilized by sonication for 6 min at high setting (30 s ON, 30 s OFF). Cellular debris was removed by centrifugation at 14 000g for 20 min at 4°C and the supernatants were collected as the chromatin fractions.

For immunoprecipitation, 5–10 mg nucleoplasmic and corresponding cytoplasmic extracts, respectively, were incubated with 5 µl anti-MSL2 (replicate A) or 2 µl anti-MSL2 serum (replicate B and C) for 45 min at 4°C with agitation. The antibody complexes were then precipitated as described above. RNA was isolated using TRI-reagent (Ambion), followed by DNase treatment using TURBO DNA-free kit (Ambion) and purification using an RNeasy kit (Qiagen) according to the manufacturer's instruction. For replicate C, poly(A)<sup>+</sup> RNA was isolated using Dynabeads Oligo (dT)<sub>25</sub> (Invitrogen) in line with the instruction by the suppliers. The RNA samples were reverse-transcribed into cDNA using iScript cDNA synthesis kit (Bio-Rad).

The RIP cDNA and the corresponding total cDNA were quantified by real-time PCR using SYBR green supermix (Bio-Rad). The primer pairs used were: *roX1* (5'-TACCGCTCTCTTTTCGGGACTTG-3', 5'-TCCATC ACTCTCTATCGGGCTG-3'), *roX2* (5'-GGCCATCGA AAGGGTAAATTG-3', 5'-ACTGTCCGTAAGACAAT TCAAC-3'), *msl2* (5'-CTGGACACGAATAGTGAA GCC-3', 5'-TTGCAGCAATCCCAGCATC-3'), *actin* (5'-CAGCCAGCAGTCGTCTAATC-3', 5'-ACAACCA GAGCAGCAACTTC-3') and *Rpl32* (5'-CGATGTTGG GCATCAGATAC-3', 5'-CCCAAGATCGTGAAGAAG C-3'). The relative enrichment levels were calculated in relation to *actin* cDNA in each replicate.

## RESULTS

To determine the potential association of the MSL complex with RNA moieties in an unbiased procedure, we performed RIP experiments on nuclear extracts from S2 cells, with and without cross-linking, followed by tiling-array analysis (RIP-chip) (Figure 1). For the RIP experiment, we chose MSL2 as a representative of the MSL-complex scaffold (consisting of MSL1 and MSL2) required for the complex to bind DNA and MOF as a representative of the complex members required for spreading (1,35).

### MSL-complex associates with *roX1* and *roX2* RNAs from the X chromosome

We first investigated the enrichment of RNAs transcribed from the X chromosome in the MSL2- and MOF-RIPs. We found that, as predicted, *roX1* and *roX2* are highly enriched in the complex (Figure 1). We found no evidence of any additional X-linked non-coding RNA associated with the MSL complex when *roX1* and *roX2* are present (Figure 1). Neither did we find any evidence that the MSL-complex attracts any cryptic RNA species produced at the MREs. The overall enrichment levels of



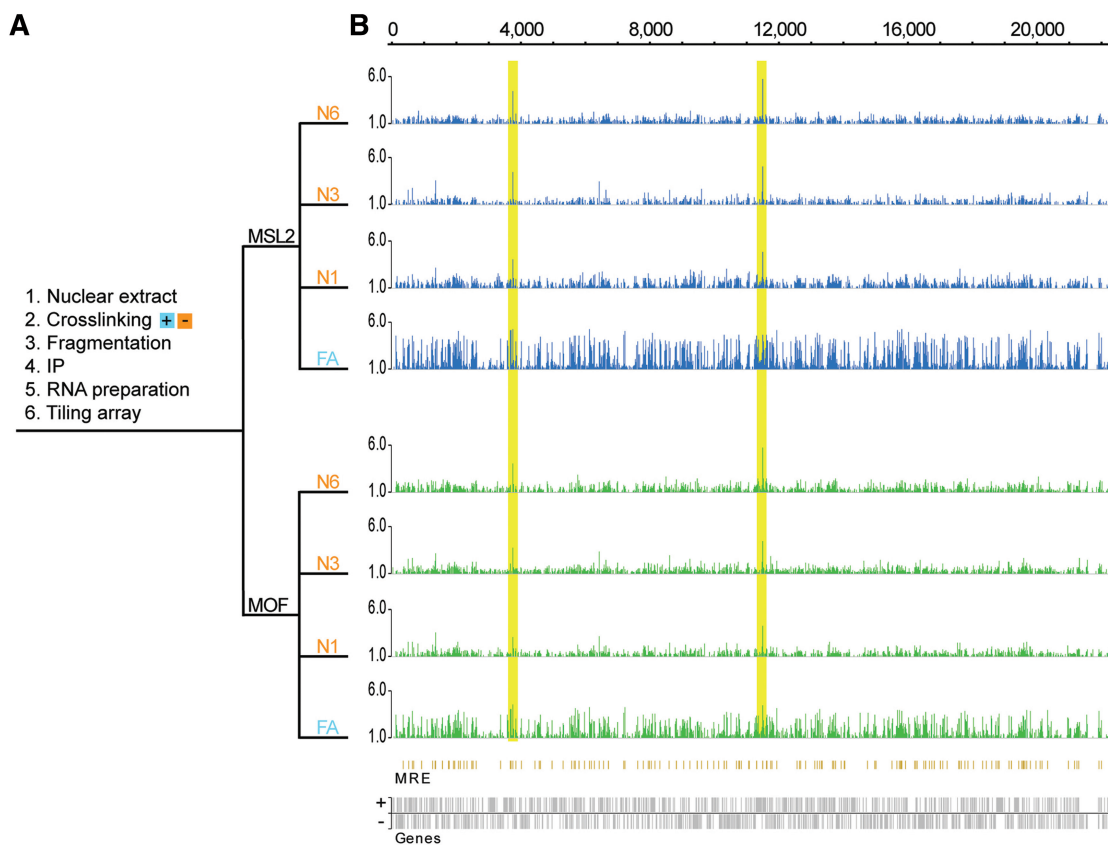


**Figure 1.** MSL-complex associates with *roX1* and *roX2* RNAs transcribed from the X chromosome. (A) Schematic outline of the RIP method. N1, N3 and N6 correspond to native nuclear extracts sonicated for 1, 3 and 6 min, respectively. FA corresponds to formaldehyde-cross-linked nuclear extract. (B) The tiling array results are computed as the ratio between the RIP value and the value of the corresponding nuclear input RNA preparation; MSL2-RIPs (blue), MOF-RIPs (green). Ratios calculated between the RIP values and a MOCK-RIP (instead of input) yield comparable results (data not shown). The plots show the mean enrichment ratios obtained using a bandwidth of 90 bp. Numbers on the x-axis denote chromosomal position along the X chromosome in kilobase. The y-axis shows the RIP enrichment as the  $\log_2$ -ratio. In the resulting profile, enrichments  $>1$  (which correspond approximately to the top 1% of binding) are shown. Genes expressed from left to right are shown above the horizontal line and genes expressed in the opposite direction are shown below the line. The high peaks within the yellow boxes are *roX1* and *roX2*, respectively. Below the enrichment plots, the MRE sites are indicated (orange) as previously characterized by (13). No significant correlation of immunoprecipitated RNAs to MREs was found.

the X chromosome and the autosomes are comparable (Supplementary Figure S1). In the formaldehyde fixed samples (FA), X chromosome transcripts in general were enriched compared with transcript on other chromosomes. We therefore compared our RIP-chip data with available ChIP-chip data representing the MSL-complex binding profile. The results showed that the RIP from the native nuclear extract is highly enriched in *roX* RNAs while the RIP experiment from the formaldehyde cross-linked nuclear extract is in addition enriched in transcripts from genes targeted by the MSL complex (Figure 2A–C). This is probably a consequence of cross-linked chromatin fragments including RNA moieties linked by active transcription.

A detailed analysis of the *roX1*- and *roX2*-precipitated RNAs shows that the entire *roX1* and *roX2* RNAs are immunoprecipitated by antibodies against both MOF and MSL2 (Figure 2D–E and Supplementary Figure S2). A higher enrichment of *roX2* compared to *roX1* was observed in all conditions except in the formaldehyde

cross-linked sample, suggesting that *roX2* is more stably bound to the complex in S2 cells.

### The MSL complex is strongly associated with nuclear *msl2* mRNA

It is well established that the *roX* genes can exert their activity in *trans* as well as in *cis* (24). We, therefore, asked whether any autosomal RNA has a stable association with the MSL complex. Visual inspection of enrichment curves readily identified a second target with a comparable enrichment ratio to *roX1* and *roX2*, namely the *msl2* transcript itself (Figure 3A). A ranking of all nuclear transcripts according to their mean enrichment ratio showed that *msl2* binding is indeed comparable with the *roX* enrichments. Furthermore, *msl1* also scored highly in this ranking, although much lower than *roX1*, *roX2* and *msl2* (Figure 3B and Supplementary Figure S3). It should be stressed that not only the enrichment ratio but also the absolute amount of *msl2* RNA pulled down with the MSL complex are comparable to *roX* levels



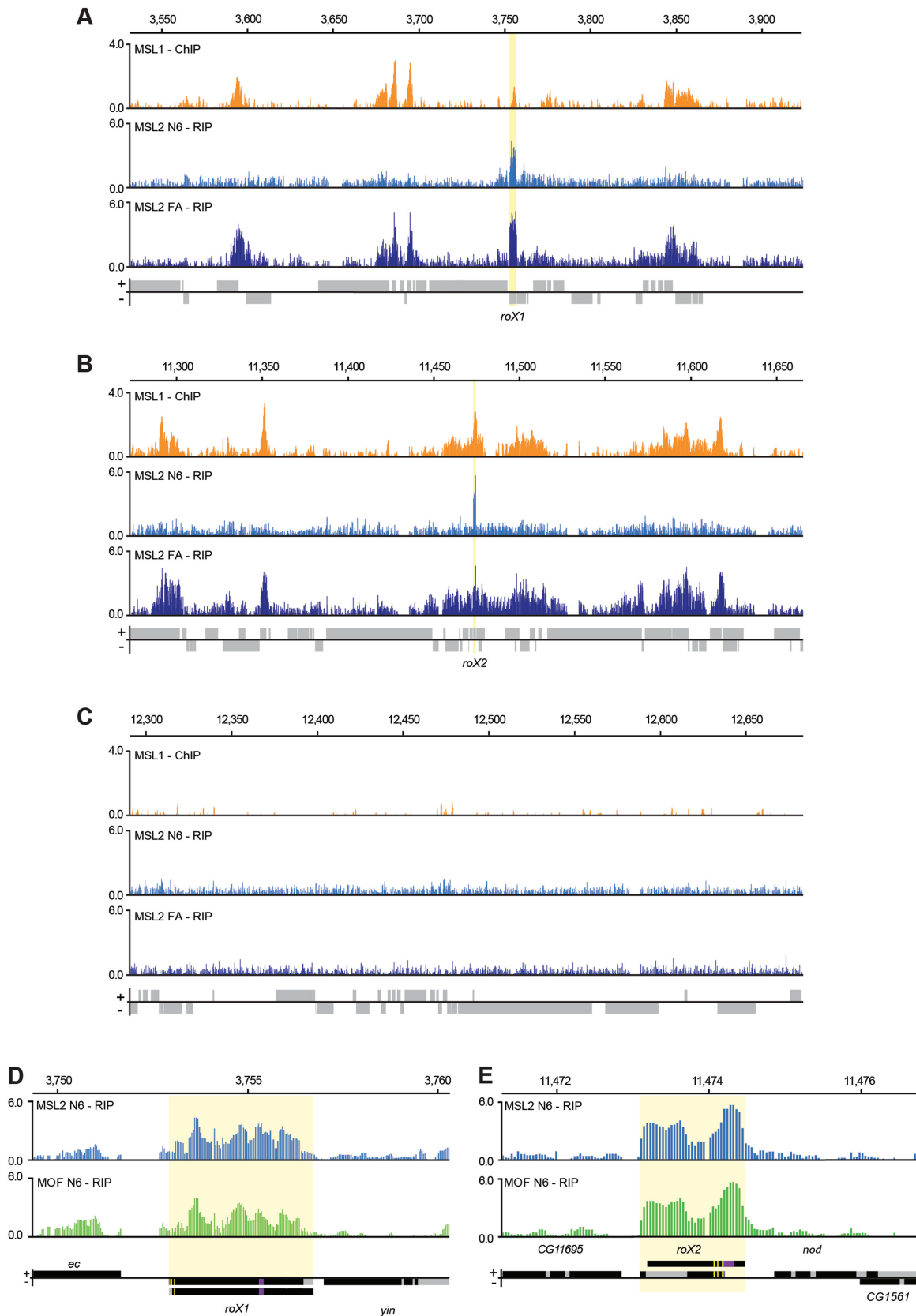


**Figure 2.** Entire *roX1* and *roX2* mRNAs are associated with a complete or partial MSL complex. (A–C) In formaldehyde cross-linked extracts, actively transcribed RNAs are immunoprecipitated by chromatin-associated proteins. Comparison of a ChIP-chip profile representing the MSL complex (MSL1-ChIP) and the MSL2 RIP-chip profiles from the native nuclear extract (MSL2 N6-RIP) and formaldehyde-cross-linked nuclear extract (MSL2 FA-RIP). Representative 400 kb regions from the X chromosome including *roX1* (A) and *roX2* (B) are compared to a representative

(continued)

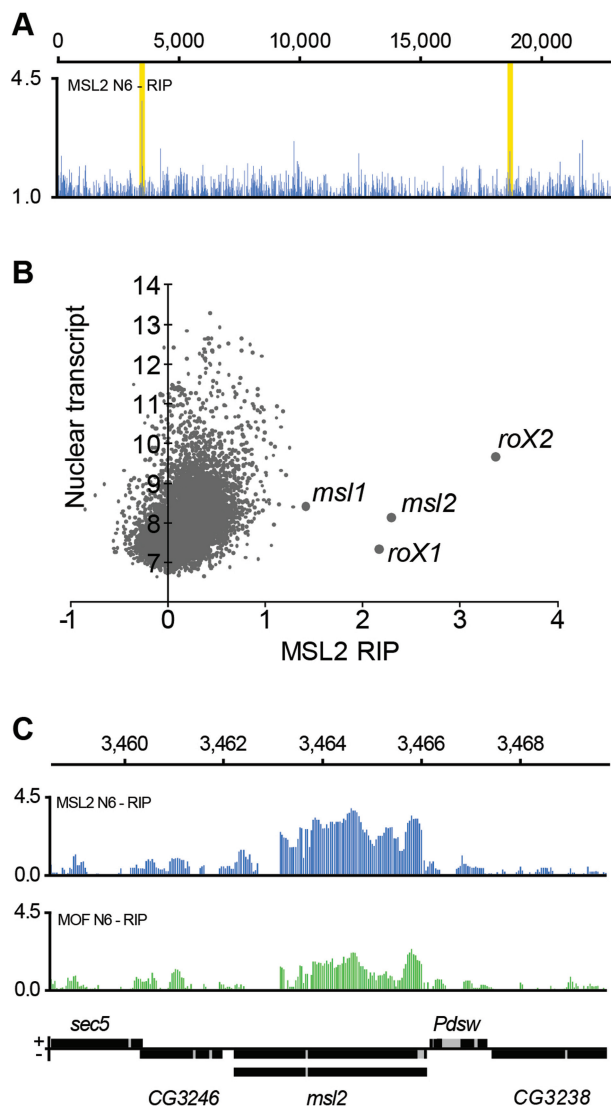


**Figure 3.** MSL complex is strongly associated with nuclear *msl2* mRNA. (A) High resolution enrichment profiling along chromosome 2L shows that *msl2* is enriched in the MSL2-RIP at similar ratios to *roX1* and *roX2*. The high peaks within the yellow boxes correspond to *msl2* (left box) and *msl1* (right box). (B) Average calculated enrichment levels of genes (*x*-axis) plotted against the average amount of nuclear transcript (*y*-axis,  $\log_2$  scale) for all genes with at least 10 probes within exons. *roX1*, *roX2* and *msl2* clearly ordinate as highly enriched. Note that the absolute amount of *msl2* RNA pulled down is similar to the absolute amounts of the *roX* RNAs. (C) The entire *msl2* mRNA is associated with a complete or partial MSL complex. High resolution enrichment profiles of MSL2-RIP (blue) and MOF-RIP (green) at the *msl2* locus. The *msl2* gene is transcribed from right to left and the different splice forms are indicated. Numbers on the *x*-axis denote chromosomal position along the X chromosome in kilobase. The *y*-axis shows the RIP enrichment as the  $\log_2$  ratio.

(Figure 3B and Supplementary Figure S3). We asked whether the *msl2* and *msl1* RNAs were pulled down by free MSL2 protein, or by MSL2 associated with the MSL complex. Notably, *roX1* and *roX2* RNAs are enriched at similar levels in both MSL2-RIP and MOF-RIP. In contrast, *msl2* RNA is enriched in both RIPs but at higher levels in the MSL2-RIP than in the MOF-RIP (compare Figure 2D–E with Figure 3C). The results suggest that *msl2* RNA is associated with a less stable MSL complex. Still, since the MOF-RIP also shows high enrichment of *msl2* and *msl1* RNA, we conclude that *msl2* and *msl1* RNAs are associated with a partial or complete nuclear MSL complex (Figure 3C and Supplementary Figure S4). We have not found any significant sequence identities or predicted secondary structure similarities between *msl2* and *roX1* or *roX2*.

#### *msl2* RNA is bound by a non-chromatin-associated MSL complex

We considered two plausible models to account for a potential function for the strong association of a nuclear complete or partial MSL complex with the *msl2* RNA. First, *msl2* may aid the correct targeting of the MSL complex, by functioning similarly to *roX*. Second, since the local concentration of MSL complex is important for spreading and therefore for the correct regulation of most X-linked genes, we can hypothesize that the non-chromatin bound fraction of the MSL complex titrates the *msl2* RNA. A combination of these two models is also possible. Recalling that the *roX* RNAs coat the male X chromosome, co-localizing with MSL complex, we performed *in situ* hybridization with RNA probes against *roX1* and *msl2*. As previously shown, *roX1* decorates the male X chromosome in a similar pattern to the MSL complex. However, we did not observe chromatin-associated *msl2* RNA in the wild-type (Figure 4A). Previously, a co-transcriptional assembly of the MSL complex at the *roX* loci has been suggested (1,27,36). In contrast, the MSL complex is not found at the *msl2* locus in published ChIP-chip analysis (Supplementary Figure S5). This indicates that the association of MSL complex with *msl2* RNA is not co-transcriptional.

We speculated that a loss of *roX1* *roX2* and/or overexpression of *msl2* may enhance an intrinsic property of the *msl2* RNA to be included in the chromatin-associated MSL complex. In *roX1* *roX2* mutant males, MSL complex is still detected at a reduced number of sites on the X chromosome, but strong binding is also reproducibly found in the

#### Figure 2. Continued

400 kb region from chromosome 3R (C). The plots show the mean enrichment ratios obtained using a bandwidth of 300 bp for the MSL1 ChIP-chip and a bandwidth of 90 bp for the MSL2 RIP-chip. Numbers on the *x*-axis denote chromosomal position along the chromosome in kb. The *y*-axis shows the ChIP and RIP enrichments, respectively, as the  $\log_2$  ratio. Genes expressed from left to right are shown above the horizontal line and genes expressed in the opposite direction are shown below the line. The *roX1* and *roX2* loci are indicated by yellow boxes. The MSL1 ChIP data is from (32). (D and E) High resolution enrichment profiles of MSL2-RIP and MOF-RIP at the *roX1* (D) or *roX2* (E) locus. Exons are indicated in black and introns in grey. The different transcript forms of *roX1* and *roX2* are indicated. The described DNase hypersensitive regions and *roX*-boxes suggested to be of functional importance (36,51–53) are indicated as deep-purple and yellow boxes, respectively. We observed a general enrichment of the entire mRNA and no obvious specificity to parts of the RNAs.

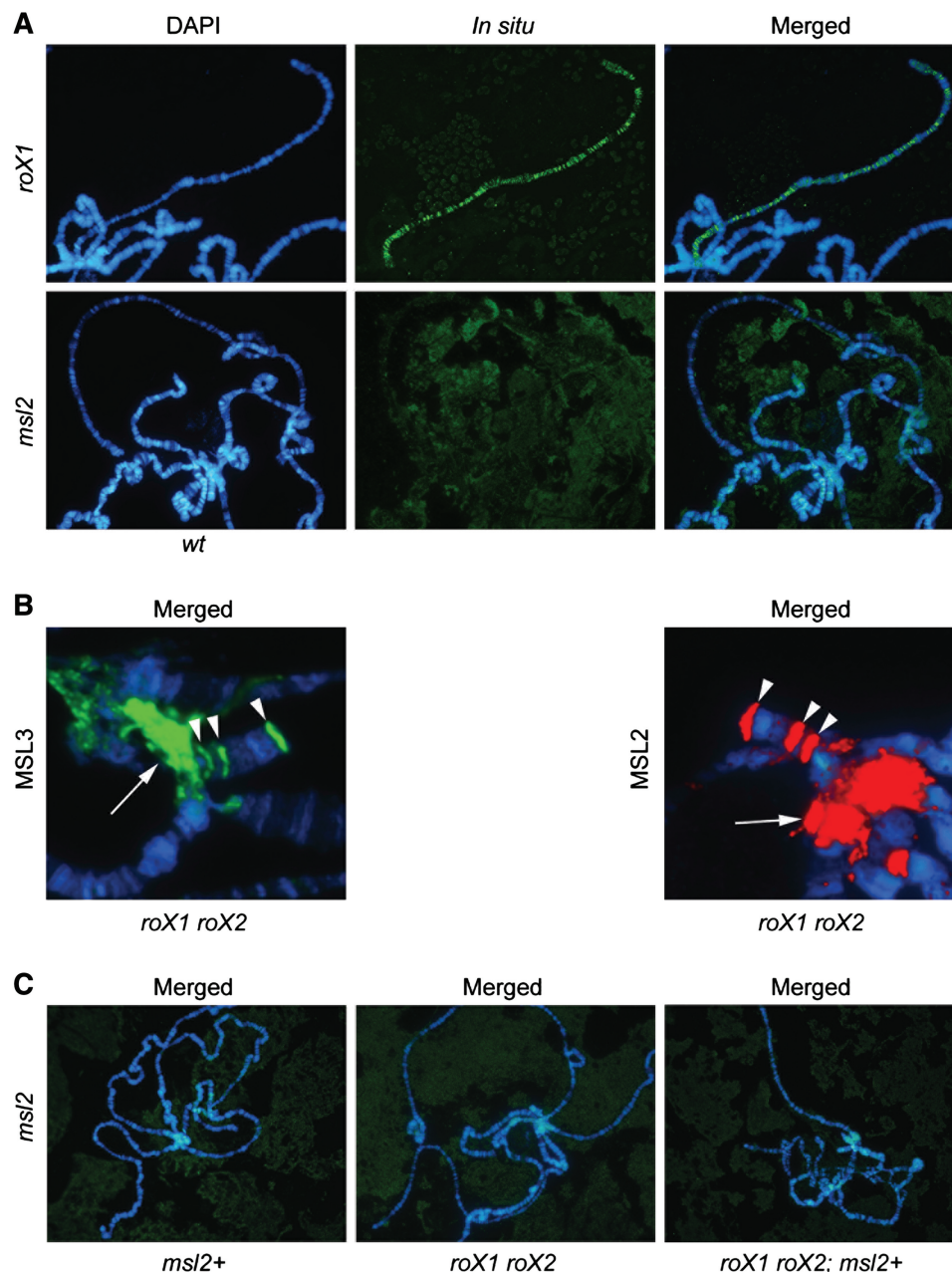


**Figure 4.** In polytene chromosomes, *msl2* RNA is not associated with the chromatin bound MSL complex. (A) *In situ* hybridization shows that *roX1* decorates the male X chromosome (top row of images). No *msl2* RNA associated with the wild-type male X chromosome is detected (bottom row of images). (B) In *roX1 roX2* mutant males MSL2 and MSL3 target the chromocenter and three specific sites on the fourth chromosome. Merged images of immunostainings showing DAPI in blue, MSL3 in green and MSL2 in red. The chromocenter is indicated by an arrow and the specific sites on the fourth chromosome with arrowheads (Supplementary Figure S6). (C) Merged images from *in situ* hybridization with *msl2* RNA antisense probe on males overexpressing *msl2* (left panel), *roX1 roX2* mutant males (middle) and *roX1 roX2* mutant males overexpressing *msl2* (right) (Supplementary Figure S8).

chromocenter and at a few specific sites on the fourth chromosome (Figure 4B and Supplementary Figure S6) (24,37). Notably, the specific sites on the fourth chromosome targeted by the MSL complex in *roX1 roX2* mutants are also targeted weakly by the MLE protein alone in wild-type, both in males and females (Supplementary Figure S7). We hybridized *roX1 roX2* mutant male larvae with and without overexpression of *msl2* and wild-type males with overexpression of *msl2*. In none of

these cases did we detect *msl2* RNA linked to the X chromosome, in the chromocenter, or the highly specific sites on the fourth chromosome (Figure 4C and Supplementary Figure S8).

In the RIP experiments performed on S2 cells a strong enrichment of *msl2* RNA in the MSL complex was detected. To test if *msl2* is included in an X chromosome-associated MSL complex in S2 cells, we performed *in situ* hybridizations on these cells (Figure 5).



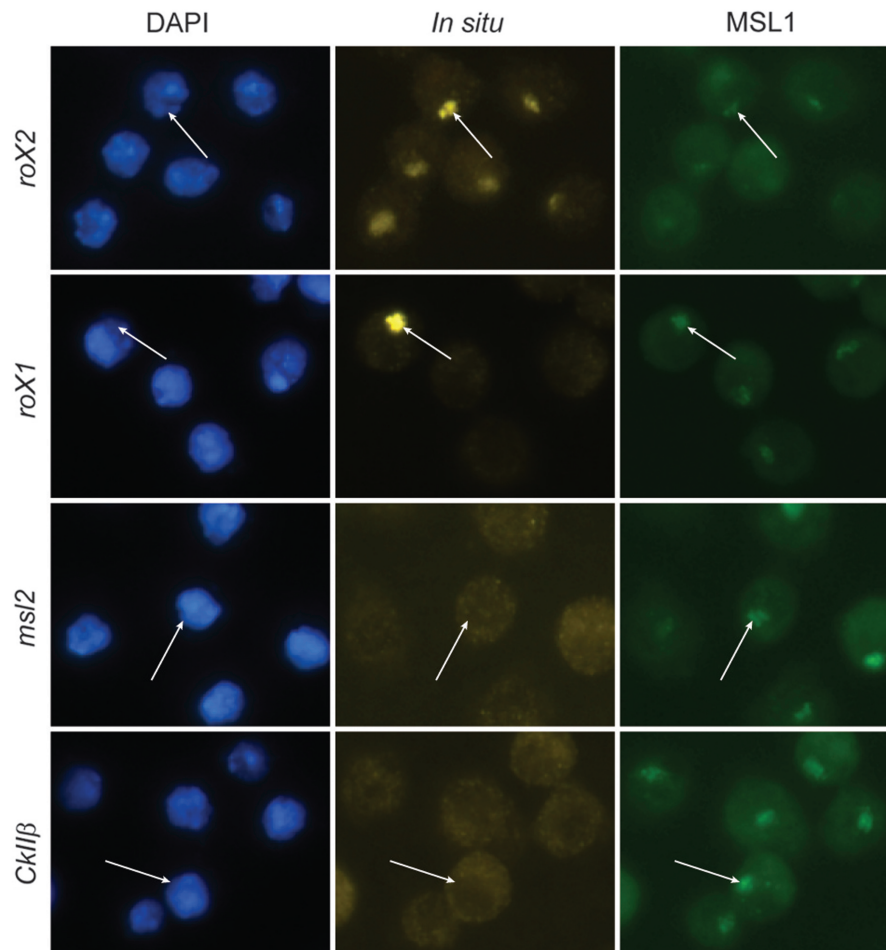


**Figure 5.** In S2 cells, *msl2* RNA is not associated with the chromatin bound MSL complex. Immunostaining and *in situ* hybridization show that *roX2* (yellow) decorates the X chromosome identified by MSL1 (green). Note that *roX1* decorates the X chromosome in a small fraction of cells (<0.5%). Nuclei are visualized with DAPI. Neither the *msl2* RNA nor the negative control *Ckl1β* RNA are enriched on the X chromosome. In each row, the location of one X chromosome in a representative cell is indicated with an arrow.

As expected, *roX2* RNAs co-localize with the MSL1 protein on the X chromosome. In agreement with the results from salivary glands we did not find any enrichment of *msl2* RNA on the X chromosome in S2 cells, indicating that the *msl2* RNA associates to a non-chromatin bound MSL complex. Strong *roX2* hybridization was observed on the X chromosome territories in all cells. Interestingly, *roX1* hybridization was as strong, but only detected in a small fraction of cells (<0.5%). This suggests that the observed low expression of *roX1* in S2 cells is due to expression in few individual cells and not a general low expression level in all cells.

Next, we performed a crude fractionation of nuclei into a chromatin fraction and a nucleoplasmic fraction and determined the relative levels of *roX1*, *roX2* and *msl2* by qPCR. The results show that the majority of both *roX1* and *roX2* RNAs are located in the chromatin fraction while the *msl2* transcripts are primarily found in the nucleoplasm (Figure 6A–C). MSL2-RIP experiments using the nucleoplasmic fractions show very strong enrichments of *roX1*, *roX2* and *msl2* RNA, verifying the nuclear RIP-chip data. Gel electrophoresis of the RIP experiment

qPCR products shows that the MSL complex-associated *msl2* RNAs are spliced. The results also show that the *msl2* RNA associated to the MSL complex is poly-adenylated, since *msl2* RNA is enriched to the same extent when using poly-adenylated RNA (Figure 6C) as when using total RNA (Figure 6A–B) in the analysis. To exclude that the enrichment of *msl2* RNA in the nucleoplasm is caused by contaminating cytoplasm, we performed MSL2-RIP also on corresponding cytoplasmic fractions. Weak enrichments of *roX* and *msl2* RNAs were detected in the cytoplasm but much lower than the enrichments found in corresponding nucleoplasm (Supplementary Figure S9). We conclude that a spliced poly-adenylated *msl2* RNA associates with a nucleoplasmic complete or partial MSL complex.

## DISCUSSION

For many chromatin-associated factors, the relative concentrations direct their binding. Thus, correct targeting will strictly depend on the concentration of these protein

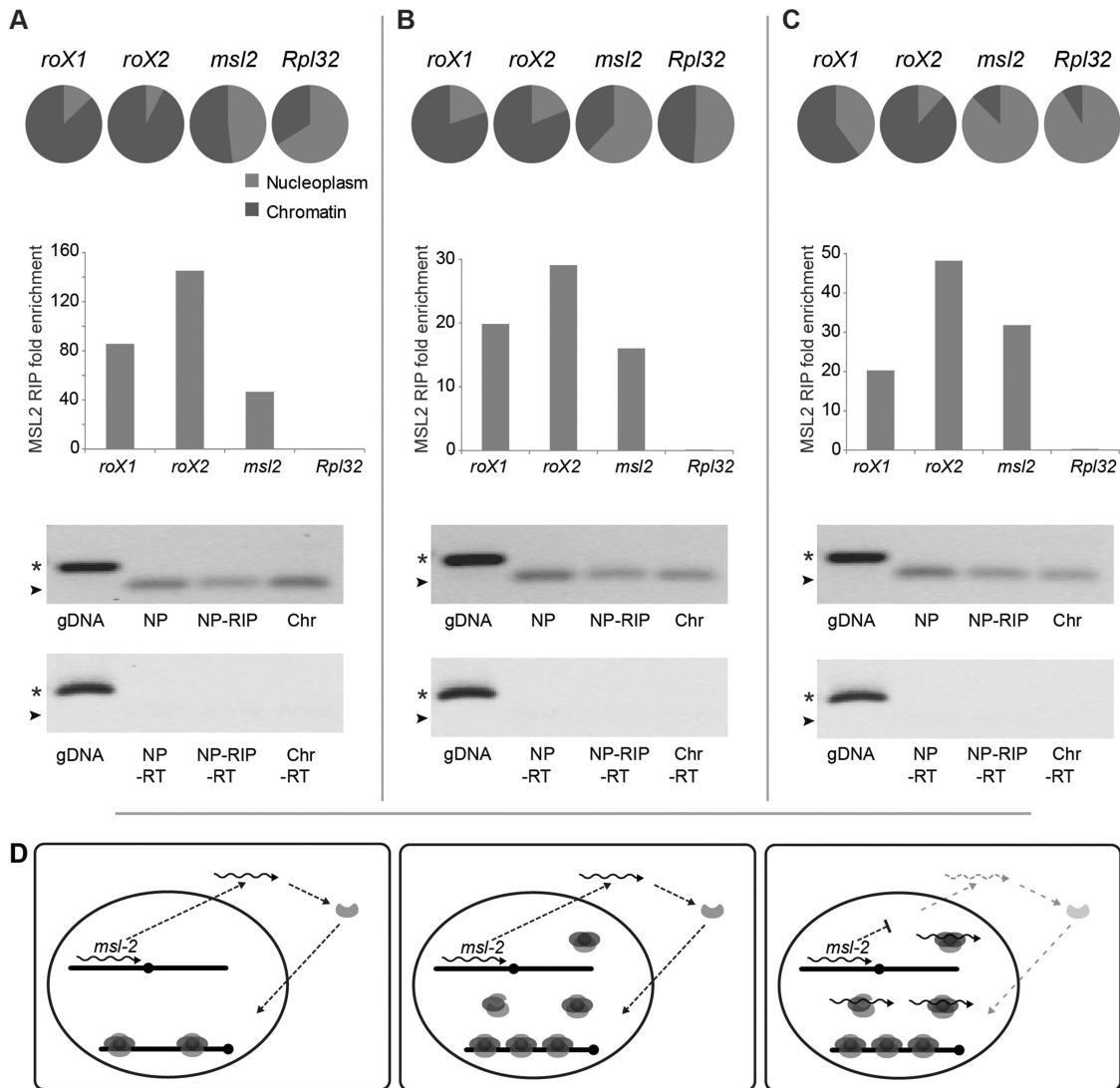


**Figure 6.** Spliced and poly-adenylated *msl2* RNA is associated to a non-chromatin bound MSL complex. (A–C) Fractionation and RIP experiments of three biological replicates using total RNA extraction (A and B) and extracted poly(A)<sup>+</sup> RNA (C). The circle diagrams specify the relative proportion of the RNAs in the nucleoplasm (gray) and the chromatin fractions (dark gray). The majority of the *roX1* and *roX2* RNAs are located in the chromatin fraction while *msl2* and the negative control *Rpl32* are mainly found within the nucleoplasm. As illustrated in the histograms, enrichment of *msl2* RNA in the MSL complex is confirmed by RIP experiments on the nucleoplasmic fractions using MSL2 antibodies. Displayed are the fold enrichments relative to *actin* RNA. Immunoprecipitated *msl2* in experiments A, B and C correspond to 3, 4 and 10% of input, respectively. Gel-electrophoretic analyses of amplified genomic DNA (gDNA), immunoprecipitated (NP RIP) and total RNA from the nucleoplasm (NP) and from chromatin (Chr) fractions show that *msl2* RNAs associated to the MSL complex are spliced. The PCR product sizes of the spliced *msl2* amplicon and the unspliced amplicon are indicated by arrowheads and stars, respectively. The minus reverse transcriptase controls (-RT) are shown below. (D) Model for feedback regulation of MSL complex via the association of a non-chromatin MSL complex with the *msl2* mRNA. When free nuclear MSL complex is present this non-chromatin MSL-complex titrates *msl2* RNA and thus reduces the amount of *msl2* transcript available for export and translation, which in turn regulates the complex production as a feedback mechanism.

complexes. It is well established that the MSL complex is restricted to males by a translational block caused by Sxl protein binding to the *msl2* transcripts. However, it has been suggested that Sxl binds not only all *msl2* transcripts, but also to a subset of *msl1* transcripts and prevents their translation in females (19). This reflects the potential of these two RNAs to be regulated through specific protein interactions. These two RNAs encode the core of the dosage compensation complex. Here, we provide evidence that a non-chromatin bound fraction of the MSL complex has high affinity for nuclear *msl2* mRNA

and also affinity for nuclear *msl1* mRNA. Based on this, we propose a novel mechanism for fine-tuning the MSL complex concentration by feedback.

We have used both formaldehyde fixed nuclear extracts and native nuclear extracts in our RIP experiments. In both these sample types, we detected strong enrichments of *roX1*, *roX2* and *msl2* transcripts. In the native extracts, we could not detect significant enrichment of RNA transcribed from genes targeted by the MSL complex nor any enrichment of RNA molecules transcribed from MREs. Although, we found robust enrichment of *roX1*

and *roX2* we did not find any additional *roX* RNA that could explain the escape of male lethality seen in *roX1 roX2* double mutants. It should be stressed that it is still possible that a *roX*-like encoding gene is harbored in the heterochromatic regions which are not fully covered by the tiling arrays. Alternatively, several different RNAs may substitute for *roX1* and *roX2* but with much lower affinity or the MSL complex can exert its function without an RNA molecule. In contrast, in the formaldehyde fixed sample we detected enrichments of transcripts from genes targeted by the MSL complex. We conclude that RIP using formaldehyde cross-linked extracts will be enriched in RNA species directly linked to the targeted protein as well as nascent RNA molecules linked via chromatin and active transcription. This is important to consider when using formaldehyde fixation in RNA immunoprecipitation experiments.

We describe two potential functions for the strong association of a nuclear MSL complex with the *msl2* RNA. First, *msl2* may aid the correct targeting of the MSL complex, by functioning similarly to *roX*. This could have been a function in a more ancient form of the MSL complex and may in part have been retained during evolution. In favour of this model is the fact that *roX1 roX2* double mutations are not completely male lethal, in contrast to *msl* mutations. The elevation of cellular levels of MSL1 and MSL2 that partially suppress *roX1 roX2* male lethality, also supports this model. Second, since the local concentration of MSL complex is important for spreading and, therefore, also for the correct regulation of most X-linked genes, we can hypothesize that the non-chromatin bound fraction of the MSL complex titrates the *msl2* RNA. Thus, this process would regulate the amount of MSL2 protein and assembled MSL complex, as a feedback mechanism.

Since the *msl2* RNA is highly enriched in a nuclear but not chromatin-associated MSL complex, we hypothesize that this interaction functions as a feedback control that avoids elevated MSL-complex levels and compensates for overshooting (Figure 6D). It has been observed that ectopic expression of an *msl2-GFP* transgene led to reduction of the endogenous MSL2 protein levels (23). This is in line with what would be predicted from a feedback mechanism as hypothesized here. The classical example of self-mRNA targeting of proteins is from *Escherichia coli*, in which the ribosomal proteins bind to their mRNA and inhibit translation. The ribosome biogenesis can thus be regulated solely through the amount of rRNA which synthesis rate becomes rate limiting for ribosome assembly. As long as the process of ribosome assembly requires ribosomal proteins, the corresponding mRNAs will escape translation inhibition (38). Intrinsic association of RNA in chromatin regulation has been reported for the yeast SET1C histone methyl transferase complex. In this case, the association is linked to co-translational assembly of the complex (39).

The dosage compensation system is under strong evolutionary pressure to respond as new genes, chromosome regions or chromosome arms join the X chromosome and it has been shown that the MSL proteins are under adaptive evolution (40). Interestingly, strong positive

selection was detected in MSL1 and MSL2 protein domains shown to be responsible for their specific targeting to the X chromosome (41,42). Positive selection has also been shown to act on the MSL binding sites (43). This means that the dosage compensation system is under constant pressure to adapt to emerging changes. The target sequences are under constant selection as are the targeting proteins, in particular MSL1 and MSL2. Thus, the concentration requirements will also need constant adjustments. A feedback module based on association of a rate limiting mRNA would provide an optimal target for evolution to act on in order to provide a dynamic fine-tuning of complex concentration, and therefore, correct targeting. This may explain the affinity of the MSL complex to both *msl1* and *msl2* RNAs which encode the core proteins for a functional complex. At limiting concentrations of freely diffusible proteins and protein complexes only the sites with highest affinity will bind while at high concentrations even sites with low affinity will bind. It should be stressed that chromatin-associated factors are often described to be highly sensitive to correct dose (44,45). This is observed for the Polycomb-group proteins involved in maintaining repression of homeotic genes (46,47) as well as for suppressors of variegation, important for heterochromatin formation (48–50). In both these cases many loci exhibit dosage effects, indicating strict dosage needs. As more RNA immunoprecipitation data are produced it is likely that the *msl2* titration reported here is just one example of a general self-affinity module important for feedback regulation.

## ACCESSION NUMBER

The microarray data reported in this article have been deposited at <http://www.ncbi.nlm.nih.gov/geo/> (Accession: GSE20249).

## SUPPLEMENTARY DATA

Supplementary Data are available at NAR Online.

## ACKNOWLEDGEMENTS

We thank M. Kuroda for antibodies, Y. Park and V. Meller for fly stocks, K. Ekström for technical assistance and members of the Larsson and Stenberg labs for stimulating discussions.

## FUNDING

This work was supported by the Carl Tryggers and Philip Sörensen Foundations (to P.S.); the Kempe Foundations (A.M.J. and A.A.); and the Swedish Research Council and Magnus Bergvalls Foundation (J.L.). Funding for open access charge: The Swedish Research Council.

*Conflict of interest statement.* None declared.



## REFERENCES

- Gelbart, M.E. and Kuroda, M.I. (2009) *Drosophila* dosage compensation: a complex voyage to the X chromosome. *Development*, **136**, 1399–1410.
- Larsson, J. and Meller, V.H. (2006) Dosage compensation, the origin and the afterlife of sex chromosomes. *Chromosome Res.*, **14**, 417–431.
- Gupta, V., Parisi, M., Sturgill, D., Nuttall, R., Doctolero, M., Dudko, O.K., Malley, J.D., Eastman, P.S. and Oliver, B. (2006) Global analysis of X-chromosome dosage compensation. *J. Biol.*, **5**, 3.
- Nguyen, D.K. and Distech, C.M. (2006) Dosage compensation of the active X chromosome in mammals. *Nat. Genet.*, **38**, 47–53.
- Zhang, Y. and Oliver, B. (2007) Dosage compensation goes global. *Curr. Opin. Genet. Dev.*, **17**, 113–120.
- Stenberg, P., Lundberg, L.E., Johansson, A.M., Rydén, P., Svensson, M.J. and Larsson, J. (2009) Buffering of segmental and chromosomal aneuploidies in *Drosophila melanogaster*. *PLoS Genet.*, **5**, e100302.
- Zhang, Y., Malone, J.H., Powell, S.K., Periwai, V., Spana, E., Macalpine, D.M. and Oliver, B. (2010) Expression in aneuploid *Drosophila* S2 cells. *PLoS Biol.*, **8**, e1000320.
- Prestel, M., Feller, C. and Becker, P.B. (2010) Dosage compensation and the global re-balancing of aneuploid genomes. *Genome Biol.*, **11**, 216.
- Hamada, F.N., Park, P.J., Gordadze, P.R. and Kuroda, M.I. (2005) Global regulation of X chromosomal genes by the MSL complex in *Drosophila melanogaster*. *Genes Dev.*, **19**, 2289–2294.
- Deng, X., Koya, S.K., Kong, Y. and Meller, V.H. (2009) Coordinated regulation of heterochromatic genes in *Drosophila melanogaster* males. *Genetics*, **182**, 481–491.
- Straub, T. and Becker, P.B. (2007) Dosage compensation: the beginning and end of generalization. *Nat. Rev. Genet.*, **8**, 47–57.
- Prestel, M., Feller, C., Straub, T., Mitlöchner, H. and Becker, P.B. (2010) The activation potential of MOF is constrained for dosage compensation. *Mol. Cell*, **38**, 815–826.
- Alekseyenko, A.A., Peng, S., Larschan, E., Gorchakov, A.A., Lee, O.K., Kharchenko, P., McGrath, S.D., Wang, C.I., Mardis, E.R., Park, P.J. *et al.* (2008) A sequence motif within chromatin entry sites directs MSL establishment on the *Drosophila* X chromosome. *Cell*, **134**, 599–609.
- Dahlsveen, I.K., Gilfillan, G.D., Shelest, V.I., Lamm, R. and Becker, P.B. (2006) Targeting determinants of dosage compensation in *Drosophila*. *PLoS Genet.*, **2**, e5.
- Gorchakov, A.A., Alekseyenko, A.A., Kharchenko, P., Park, P.J. and Kuroda, M.I. (2009) Long-range spreading of dosage compensation in *Drosophila* captures transcribed autosomal genes inserted on X. *Genes Dev.*, **23**, 2266–2271.
- Larschan, E., Alekseyenko, A.A., Gorchakov, A.A., Peng, S., Li, B., Yang, P., Workman, J.L., Park, P.J. and Kuroda, M.I. (2007) MSL complex is attracted to genes marked by H3K36 trimethylation using a sequence-independent mechanism. *Mol. Cell*, **28**, 121–133.
- Sass, G.L., Pannuti, A. and Lucchesi, J.C. (2003) Male-specific lethal complex of *Drosophila* targets activated regions of the X chromosome for chromatin remodeling. *Proc. Natl Acad. Sci. USA*, **100**, 8287–8291.
- Bashaw, G.J. and Baker, B.S. (1997) The regulation of the *Drosophila msl-2* gene reveals a function for Sex-lethal in translational control. *Cell*, **89**, 789–798.
- Kelley, R.L., Solovyeva, I., Lyman, L.M., Richman, R., Solovyev, V. and Kuroda, M.I. (1995) Expression of *msl-2* causes assembly of dosage compensation regulators on the X chromosomes and female lethality in *Drosophila*. *Cell*, **81**, 867–877.
- Kelley, R.L., Wang, J., Bell, L. and Kuroda, M.I. (1997) Sex lethal controls dosage compensation in *Drosophila* by a non-splicing mechanism. *Nature*, **387**, 195–199.
- Chang, K.A. and Kuroda, M.I. (1998) Modulation of MSL1 abundance in female *Drosophila* contributes to the sex specificity of dosage compensation. *Genetics*, **150**, 699–709.
- Deng, X., Rattner, B.P., Souter, S. and Meller, V.H. (2005) The severity of *roX1* mutations is predicted by MSL localization on the X chromosome. *Mech. Dev.*, **122**, 1094–1105.
- Straub, T., Neumann, M.F., Prestel, M., Kremmer, E., Kaether, C., Haass, C. and Becker, P.B. (2005) Stable chromosomal association of MSL2 defines a dosage-compensated nuclear compartment. *Chromosoma*, **114**, 352–364.
- Meller, V.H. and Rattner, B.P. (2002) The *roX* genes encode redundant male-specific lethal transcripts required for targeting of the MSL complex. *EMBO J.*, **21**, 1084–1091.
- Menon, D.U. and Meller, V.H. (2009) Imprinting of the Y chromosome influences dosage compensation in *roX1 roX2 Drosophila melanogaster*. *Genetics*, **183**, 811–820.
- Ilik, I. and Akhtar, A. (2009) *roX* RNAs: non-coding regulators of the male X chromosome in flies. *RNA Biol.*, **6**, 113–121.
- Oh, H., Park, Y. and Kuroda, M.I. (2003) Local spreading of MSL complexes from *roX* genes on the *Drosophila* X chromosome. *Genes Dev.*, **17**, 1334–1339.
- Fujii, S. and Amrein, H. (2002) Genes expressed in the *Drosophila* head reveal a role for fat cells in sex-specific physiology. *EMBO J.*, **21**, 5353–5363.
- Larsson, J., Chen, J.D., Rasheva, V., Rasmuson Lestander, A. and Pirrotta, V. (2001) Painting of fourth, a chromosome-specific protein in *Drosophila*. *Proc. Natl Acad. Sci. USA*, **98**, 6273–6278.
- White, R.A.H. (1998) Immunolabelling of *Drosophila*. In Roberts, D.B. (ed.), *Drosophila, a practical approach*. IRL Press, Oxford, pp. 215–240.
- Meller, V.H., Gordadze, P.R., Park, Y., Chu, X., Stuckenholz, C., Kelley, R.L. and Kuroda, M.I. (2000) Ordered assembly of *roX* RNAs into MSL complexes on the dosage-compensated X chromosome in *Drosophila*. *Curr. Biol.*, **10**, 136–143.
- Kind, J., Vaquerizas, J.M., Gebhardt, P., Gentzel, M., Luscombe, N.M., Bertone, P. and Akhtar, A. (2008) Genome-wide analysis reveals MOF as a key regulator of dosage compensation and gene expression in *Drosophila*. *Cell*, **133**, 813–828.
- Tweedie, S., Ashburner, M., Falls, K., Leyland, P., McQuilton, P., Marygold, S., Millburn, G., Osumi-Sutherland, D., Schroeder, A., Seal, R. *et al.* (2009) FlyBase: enhancing *Drosophila* Gene Ontology annotations. *Nucleic Acids Res.*, **37**, D555–D559.
- Aygün, O., Svejstrup, J. and Liu, Y. (2008) A RECQ5-RNA polymerase II association identified by targeted proteomic analysis of human chromatin. *Proc. Natl Acad. Sci. USA*, **105**, 8580–8584.
- Lucchesi, J.C., Kelly, W.G. and Panning, B. (2005) Chromatin remodeling in dosage compensation. *Annu. Rev. Genet.*, **39**, 615–651.
- Kelley, R.L., Lee, O.K. and Shim, Y.K. (2008) Transcription rate of noncoding *roX1* RNA controls local spreading of the *Drosophila* MSL chromatin remodeling complex. *Mech. Dev.*, **125**, 1009–1019.
- Deng, X. and Meller, V.H. (2006) *roX* RNAs are required for increased expression of X-linked genes in *Drosophila melanogaster* males. *Genetics*, **174**, 1859–1866.
- Nomura, M., Gourse, R. and Baughman, G. (1984) Regulation of the synthesis of ribosomes and ribosomal components. *Annu. Rev. Biochem.*, **53**, 75–117.
- Halbach, A., Zhang, H., Wengi, A., Jablonska, Z., Gruber, I.M., Halbeisen, R.E., Dehè, P.M., Kemmeren, P., Holstege, F., Géli, V. *et al.* (2009) Cotranslational assembly of the yeast SET1C histone methyltransferase complex. *EMBO J.*, **28**, 2959–2970.
- Bachtrog, D., Jensen, J.D. and Zhang, Z. (2009) Accelerated adaptive evolution on a newly formed X chromosome. *PLoS Biol.*, **7**, e82.
- Levine, M.T., Holloway, A.K., Arshad, U. and Begun, D.J. (2007) Pervasive and largely lineage-specific adaptive protein evolution in the dosage compensation complex of *Drosophila melanogaster*. *Genetics*, **177**, 1959–1962.
- Rodriguez, M.A., Vermaak, D., Bayes, J.J. and Malik, H.S. (2007) Species-specific positive selection of the male-specific lethal complex that participates in dosage compensation in *Drosophila*. *Proc. Natl Acad. Sci. USA*, **104**, 15412–15417.
- Bachtrog, D. (2008) Positive selection at the binding sites of the male-specific lethal complex involved in dosage compensation in *Drosophila*. *Genetics*, **180**, 1123–1129.
- Veitia, R.A. (2002) Exploring the etiology of haploinsufficiency. *BioEssays*, **24**, 175–184.

45. Edger,P.P. and Pires,J.C. (2009) Gene and genome duplications: the impact of dosage-sensitivity on the fate of nuclear genes. *Chromosome Res.*, **17**, 699–717.
46. Kennison,J.A. and Russell,M.A. (1987) Dosage-dependent modifiers of homoeotic mutations in *Drosophila melanogaster*. *Genetics*, **116**, 75–86.
47. Campbell,R.B., Sinclair,D.A., Couling,M. and Brock,H.W. (1995) Genetic interactions and dosage effects of Polycomb group genes of *Drosophila*. *Mol. Gen. Genet.*, **246**, 291–300.
48. Henikoff,S. (1996) Dosage-dependent modification of position-effect variegation in *Drosophila*. *BioEssays*, **18**, 401–409.
49. Tartof,K.D., Bishop,C., Jones,M., Hobbs,C.A. and Locke,J. (1989) Towards an understanding of position effect variegation. *Dev. Genet.*, **10**, 162–176.
50. Locke,J., Kotarski,M.A. and Tartof,K.D. (1988) Dosage-dependent modifiers of position effect variegation in *Drosophila* and a mass action model that explains their effect. *Genetics*, **120**, 181–198.
51. Kageyama,Y., Mengus,G., Gilfillan,G., Kennedy,H.G., Stuckenholtz,C., Kelley,R.L., Becker,P.B. and Kuroda,M.I. (2001) Association and spreading of the *Drosophila* dosage compensation complex from a discrete *roX1* chromatin entry site. *EMBO J.*, **20**, 2236–2245.
52. Park,Y., Mengus,G., Bai,X., Kageyama,Y., Meller,V.H., Becker,P.B. and Kuroda,M.I. (2003) Sequence-specific targeting of *Drosophila roX* genes by the MSL dosage compensation complex. *Mol. Cell*, **11**, 977–986.
53. Park,S.W., Kuroda,M.I. and Park,Y. (2008) Regulation of histone H4 Lys16 acetylation by predicted alternative secondary structures in *roX* noncoding RNAs. *Mol. Cell. Biol.*, **28**, 4952–4962.